ISSN 1070-3284, Russian Journal of Coordination Chemistry, 2020, Vol. 46, No. 6, pp. 386–393. © Pleiades Publishing, Ltd., 2020.
Russian Text © The Author(s), 2020, published in Koordinatsionnaya Khimiya, 2020, Vol. 46, No. 6, pp. 340–348.

The authors congratulate Academician I.L. Eremenko with a 70th birthday

Triphenylantimony(V) Catecholates Based on 3,6-Di-*tert*-Butyl-2,5-Dihydroxy-1,4-Benzoquinone

L. S. Okhlopkova[a], A. I. Poddel'sky[a, *], I. V. Smolyaninov[b], and G. K. Fukin[a]

[a] *Razuvaev Institute of Organometallic Chemistry, Russian Academy of Sciences, Nizhny Novgorod, Russia*
[b] *Southern Scientific Center, Russian Academy of Sciences, Rostov-on-Don, Russia*
**e-mail: aip@iomc.ras.ru*

Received November 5, 2019; revised December 10, 2019; accepted December 16, 2019

Abstract—2,5-Dihydroxy-3,6-di-*tert*-butyl-*p*-benzoquinone ($Q^{tBu}Diol$) reacts with Ph_3SbBr_2 in toluene in the presence of triethylamine to yield the ionic complex $[Et_3NH]^+[(Dione^{tBu}Diolate)SbPh_3Br]^-$ (**I**). The same reaction in methanol leads to complete displacement of bromide ions from the antimony coordination sphere and gives triphenylantimony(V) 1,2-diolate $(Dione^{tBu}Diolate)SbPh_3 \cdot MeOH$ (**II** · MeOH). The molecular structure of the complexes was determined by X-ray diffraction (CIF files CCDC no. 1960681 (**I** · toluene) and 1960682 (**II** · 2MeOH)). Both complexes are characterized by quinoid bond distribution in the six-membered carbon rings and by C=O double bonds in the $Ph_3SbO_2C_6(t\text{-}Bu)_2O_2$ moieties. Formally, the complexes can be considered as 3,6-di-*tert*-butyl-*o*-benzoquinone derivatives with the organometallic Ph_3SbO_2 group in positions 4 and 5 of the quinone ring. The electrochemical reduction of **II** · MeOH in dichloromethane occurs at $E_{1/2} = -1.52$ V, which is significantly shifted to the cathodic region relative to the data for 3,6-di-*tert*-butyl-*o*-benzoquinone ($E_{1/2} = -0.51$ V). This redox potential shift indicates a significant decrease in the electron-withdrawing properties of the *o*-quinoid moiety, which is caused by the effect of the electron-donating catecholate metallacycle.

Keywords: redox-active ligand, antimony, *p*-benzoquinone, diolate, catecholate, X-ray diffraction analysis, cyclic voltammetry

DOI: 10.1134/S107032842005005X

The interest in coordination compounds that can potentially act as building blocks for the design of heterometallic complexes, including coordination polymers, has greatly increased in the last decade. This is due to the fact that, first, enzymes with several metals in the active moiety are often responsible in Nature for chemical transformations requiring the transfer of one or several electrons and are involved in important processes such as oxidation, reduction, hydrolysis, etc. Examples include oxidation of water with Photosystem II [1], reduction of O_2 with cytochrome oxidase [2], N_2 fixation [3], disproportionation of the superoxide radical anion to give oxygen (superoxide dismutase), hydrogen peroxide decomposition (catalase) under the action of antioxidant protective enzymes [4], hydrolysis of phosphoric acid esters by phosphatases [5], etc. Second, heterometallic coordination compounds are actively used in various fields ranging from catalysis to medicine [6–10]. Good opportunities for producing mono-, bi-, and polynuclear homo- and heterometallic complexes are provided by 2,5-dihydroxy-1,4-benzoquinones and their 3,6-disubstituted derivatives [11–16]. However, it is noteworthy that virtually no transition metal complexes based on 3,6-di-*tert*-butyl-2,5-dihydoxy-1,4-benzoquinone have been reported [17, 18] and no data on main group metal derivatives with this ligand are available from the literature.

Here, we describe mononuclear triphenylantimony(V) complexes based on 2,5-dihydoxy-3,6-di-*tert*-butyl-1,4-benzoquinone ($Q^{tBu}Diol$). Triarylantimony(V) catecholate complexes are compounds with redox active ligand, which are of interest for several reasons: triarylantimony(III) forms rather stable chelate rings with *o*-quinones, which allows studying the chemical and electrochemical transformations of redox-active ligands without participation of the redox-inert organometallic moiety; the presence of a heavy antimony atom in the complex with a redox-active ligand allows, in some cases, modeling of the chemical behavior of transition metal complexes; antimony(V) catecholate complexes were found to exist as a variety of structural types, depending on both the structure of substituents at the central antimony atom and the structure of redox-active ligands [19]. Data on the heterometallic antimony complexes in which the

metal centers are bridged by a redox-active ligand and on mononuclear antimony catecholates, capable of acting as precursors for these heterometallic derivatives, are scarce [20–24].

EXPERIMENTAL

The synthesis, isolation, and investigation of the complexes were carried out in evacuated tubes without oxygen. The organic solvents used in the study were purified by standard procedures [25].

Synthesis of triethylammonium (3,6-di-*tert*-butylcyclohexa-1,5-diene-4,5-dione-1,2-diolate)triphenylbromoantimonate(V) $[Et_3NH]^+[(Dione^{tBu}Diolate)\text{-}SbPh_3Br]^-$ (I). A solution of triphenylantimony tribromide (100 mg, 0.2 mmol) in toluene (20 mL) was added with continuous stirring to a solution of Q^{tBu}Diol (50.8 mg, 0.2 mmol) in toluene (30 mL) in the presence of Et_3N (0.028 mL, 0.2 mmol). Almost immediately, the solution color changed to violet. Fast concentration of the solution gave complex **I** as a violet finely crystalline powder. The yield of **I** was 138 mg (91%).

For $C_{38}H_{49}NO_4BrSb$

Anal. calcd., %	C, 58.09;	H, 6.24;	Sb, 15.54.
Found, %	C, 58.05;	H, 6.28;	Sb, 15.53.

IR (Nujol; ν, cm^{-1}): 1613 s, 1530 s, 1430 s, 1394 s, 1362 s, 1303 s, 1231 m, 1212 s, 1205 s, 1185 m, 1159 m, 1068 s, 1036 w, 1022 m, 999 m, 979 m, 903 s, 840 m, 810 w, 792 w, 780 w, 733 s, 692 s, 655 s, 603 s, 557 w, 535 w, 509 w, 467 s, 454 s. ^{1}H NMR ($CDCl_3$; δ, ppm): 1.26–1.35 (m, 27 H: 18 H, CH_3, *t*Bu + 9 H, CH_3, Et_3N), 4.11 (sept., 6 H, CH_2, Et_3N), 7.15–7.35 (m, 15H, 3Ph), 7.74 (s, NH).

After slow concentration and keeping in air for a long period (3 days) at 0°C, violet crystals of complex **I** · toluene suitable for X-ray diffraction were isolated from the solution.

Synthesis of (3,6-di-*tert*-butyl-cyclohexa-1,5-diene-4,5-dione-1,2-diolate)-methanol-triphenylantimony(V) $(Dione^{tBu}Diolate)SbPh_3$ · 2MeOH (II · 2MeOH). The crimson-colored crystals of complex **II** · 2MeOH were prepared from triphenylantimony dibromide (100 mg, 0.2 mmol) and Q^{tBu}Diol (50.8 mg, 0.2 mmol) in methanol (30 mL) in the presence of triethylamine (0.2 mmol). The crystals of **II** · 2MeOH precipitated directly from the reaction mixture after complete mixing of the reactants at room temperature. The yield of **II** · 2MeOH was 111 mg (83%).

For $C_{34}H_{41}O_6Sb$

Anal. calcd., %	C, 61.18	H, 6.19	Sb, 18.24
Found, %	C, 61.29	H, 6.30	Sb, 18.02

IR (Nujol; ν, cm^{-1}): 1654 w, 1625 s, 1550 s, 1391 s, 1351 s, 1288 s, 1232 m, 1213 m, 1187 m, 1159 m, 1072 m, 1065 m, 1055 m, 1034 s, 1013 s, 997 m, 981 m, 933 w, 903 s, 825 w, 743 m, 733 s, 694 s, 655 m, 621 s, 577 m, 541 w, 501 w. ^{1}H NMR ($CDCl_3$; δ, ppm): 1.32 (s, 18 H, CH_3, *t*-Bu), 7.13–7.20 (m, 9H, *o*,*p*-H, Ph), 7.29–7.37 (m, 6 H, *m*-H, Ph). $^{13}C\{^1H\}$ NMR ($CDCl_3$; δ, ppm): 30.46, 34.24, 118.69, 125.24, 128.12, 128.98, 129.19, 134.24, 137.82.

^{1}H and $^{13}C\{^1H\}$ NMR spectra were recorded on a Bruker AVANCE DPX-200 spectrometer in $CDCl_3$. IR spectra were measured on a FSM 1201 FT IR spectrometer in Nujol. Elemental analysis was carried out on a Euro EA 3000 C,H,N analyzer and by pyrolytic decomposition in an oxygen flow. Quantum chemical calculations were performed using the Gaussian09 software package [26] by the B3LYP/def2tzvp method. The oxidation potentials were measured by cyclic voltammetry (CV) in a three-electrode cell in argon using an IPC-pro potentiostat. A stationary glass carbon working electrode (2 mm in diameter) and a platinum plate as the auxiliary electrode (S = 18 mm^2) were used. The Ag/AgCl/KCl(sat.) reference electrode with a water-tight diaphragm was employed. The potential sweep rate was 0.2 V/s.

The X-ray diffraction study of I · toluene and II · 2MeOH was carried out at 100 K on Bruker Smart Apex (**I** · toluene) and Xcalibur (**II** · 2MeOH) diffractometers (graphite monochromator, MoK_α radiation, λ = 0.71073 Å). The experimental sets of reflection intensities were integrated using the SAINT [27] and CrysAlisPro 1.171.38.46 [28] programs. The SADABS [29] and SCALE3 ABSPACK [30] were used to apply absorption corrections. The structures were solved with direct methods and refined by full-matrix least squares method on F^2 using the SHELXTL software package [31]. All non-hydrogen atoms were refined in the anisotropic approximation. The hydrogen atoms were placed into geometrically calculated positions and refined isotropically in the riding model. The crystallographic data for compounds **I** · toluene and **II** · 2MeOH are given in Table 1 and selected bond lengths are presented in Table 2.

The structural data for the crystals of **I** · toluene and **II** · 2MeOH are deposited with the Cambridge Crystallographic Data Centre (CCDC nos. 1960681 and 1960682, respectively; deposit@ ccdc.cam.ac.uk; www: http://www.ccdc.cam.ac.uk).

RESULTS AND DISCUSSION

The oxidative addition of *o*-quinones to triaryl- and trialkylstibines is a convenient synthetic approach to triorganylantimony(V) catecholates [32–38]. In most cases, this reaction proceeds without complications and affords the target product in a

Table 1. Crystal data and X-ray experiment and structure refinement details of **I** · toluene and **II** · 2MeOH

Parameter	Value	
	I · $C_6H_5CH_3$	**II** · 2MeOH
Molecular formula	$C_{45}H_{57}NO_4BrSb$	$C_{34}H_{41}O_6Sb$
M	877.57	667.42
T, K	100(2)	100(2)
System	Monoclinic	Monoclinic
Space group	$P2_1/n$	$C2/c$
a, Å	9.8072(16)	27.9065(5)
b, Å	18.541(3)	9.59000(10)
c, Å	23.146(4)	23.7840(4)
β, deg	99.487(7)	96.167(2)
V, Å	4151.1(12)	6328.32(17)
Z	4	8
ρ(calcd.), g cm^{-3}	1.404	1.401
μ, mm^{-1}	1.669	0.914
F(000)	1808	2752
Range of measurements for θ, deg	1.415–28.999	3.060–27.994
Number of collected reflections	32140	53375
Number of unique reflections	11024	7637
R_{int}	0.0701	0.0213
GOOF on F^2	1.021	1.069
R_1/wR_2 ($I > 2\sigma(I)$)	0.0570/0.1058	0.0193/0.0431
R_1/wR_2 (for all parameters)	0.0997/0.1194	0.0218/0.0439
$\Delta\rho_{max}/\Delta\rho_{min}$, e Å^{-3},	1.129/–1.291	0.412/–0.461

high (nearly quantitative) yield. Unlike *o*-quinones, 2,5-dihydoxy-3,6-di-*tert*-butyl-*p*-benzoquinone does not react with triphenylantimony in low-polarity solvents (such as toluene). However, this *p*-benzoquinone reacts with Ph_3SbBr_2 in toluene in the presence of triethylamine virtually immediately as the reactants are mixed (Scheme 1) to give ionic complex **I**.

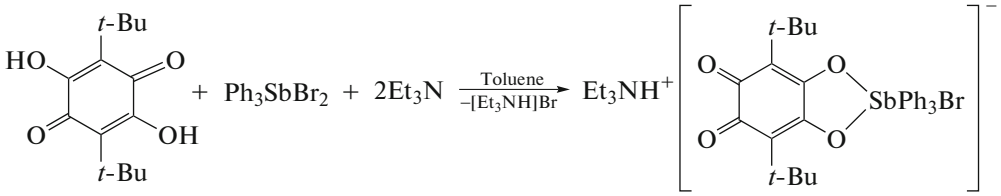

(I)

Scheme 1.

During the reaction, the reaction mixture color changes from yellow to violet. After separation of triethylammonium bromide and fast solvent evaporation, complex **I** was isolated as a crimson-colored fine powder in a nearly quantitative yield. Slow concentration of the solution and keeping at 0°C for 3 days yielded crystals of **I** · toluene suitable for X-ray diffraction. Complex **I** contains a complex anion with a bromine atom at the central antimony atom and a triethylammonium cation.

It is worth noting that replacement of toluene used as the solvent by methanol readily gives complex **II** · MeOH (Scheme 2), which does not contain a complexed ammonium salt.

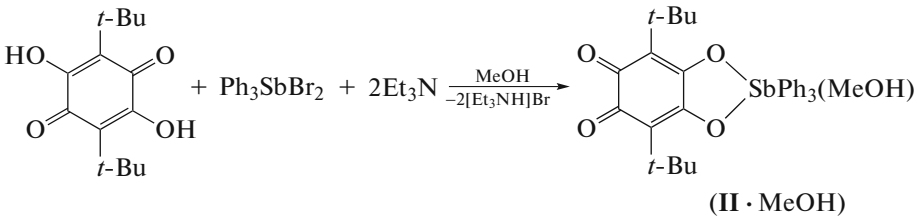

Scheme 2.

The IR spectrum of diolate **II** · MeOH in the 1200–1700 cm^{-1} frequency range exhibits intense absorption bands at 1625 and 1550 cm^{-1} and also at 1288 cm^{-1}. The first two bands correspond to carbonyl stretching modes, while the third band is typical of C–O single bonds of the diolate ligand. The Sb–C(Ph) stretching modes occur at 450–500 cm^{-1}, while the skeletal vibrations of the $SbPh_3$ moiety are manifested at 620–730 cm^{-1}. Formally, complex **II** can be considered as 3,6-di-*tert*-butyl-*o*-benzoquinone with the Ph_3SbO_2 group in positions 4 and 5 of the quinone ring.

The complexes **I** · toluene and **II** · 2MeOH were studied by single crystal X-ray diffraction. The corresponding molecular structures are shown in Fig. 1.

The structures of the coordination units in the two complexes are similar. The antimony atoms have a distorted octahedral environment formed by the O(1), O(2), C(15), C(21), and C(27) atoms and the Br(1) atom (**I**) or O(1S) atom of the coordinated methanol molecule (**II** · MeOH). The metal deviation from the equatorial plane formed by the O(1) and O(2) atoms of the catecholate ligand and the carbon atoms of two phenyl groups is 0.16(1) Å for **I** and 0.29(1) Å for **II** · MeOH. The five-membered SbOOCC metallacycle is nonplanar, with the folding angle along the O(1)...O(2) line relative to the catecholate plane being 8.5(2)° for **I** and 4.1(1)° for **II** · MeOH. Note that in the case of complex **II** · MeOH, the *tert*-butyl groups are in the staggered conformation and the carbonyl oxygens are disordered, which is not the case for the ionic derivative.

Table 2. Selected bond lengths of molecules **I** and **II** · MeOH in the crystals of **I** · toluene and **II** · 2MeOH, respectively

Bond	**I**	**II** · MeOH
	d, Å	
Sb(1)–O(1)	2.088(3)	2.059(1)
Sb(1)–O(2)	2.096(3)	2.053(1)
Sb(1)–C(15)	2.142(4)	2.128(1)
Sb(1)–C(21)	2.142(4)	2.130(1)
Sb(1)–C(27)	2.151(4)	2.135(1)
C(1)–O(1)	1.305(4)	1.318(2)
C(2)–O(2)	1.301(4)	1.311(2)
C(4)–O(3)	1.226(4)	1.233(2)
C(5)–O(4)	1.241(4)	1.229(2)
C(1)–C(2)	1.516(5)	1.525(2)
C(1)–C(6)	1.381(5)	1.369(2)
C(2)–C(3)	1.370(5)	1.366(2)
C(3)–C(4)	1.446(5)	1.438(2)
C(4)–C(5)	1.565(6)	1.550(2)
C(5)–C(6)	1.435(5)	1.451(2)
Sb(1)–Br(1)	2.6960(6)	
Sb(1)–O(1S)		2.314(1)

The C(1)–O(1) and C(2)–O(2) bond lengths (1.305(4), 1.301(4) Å in **I**; 1.318(2), 1.311(2) Å in **II** · MeOH) are in the range typical of C–O single bonds in various antimony(V) catecholate complexes [39–49], whereas the C(4)–O(3) and C(5)–O(4) bond lengths (1.226(4), 1.241(4) Å in **I**; 1.233(2), 1.229(2) Å in **II** · MeOH) are in the range typical of C=O double bonds [50]. The C(5)–O(4) bond in **I** is somewhat elongated relative to C(4)–O(3), probably, due to the fact that the triethylammonium cation in **I** is arranged in such a way that the H(1) hydrogen atom resides between the diolate ligand C=O bonds of the complex anion, pointing towards these bonds, with the H(1)...O(4) distance being 0.03 Å shorter than H(1)...O(3) (1.892(5) and 2.322(5) Å, respectively). There are four structures of this type among transition metal complexes based on 3,6-dichloro(bromo)-2,5-di-*tert*-butyl-*p*-benzoquinone, particularly, the mononuclear monoligand rhodium complex $[Et_3NH]^+[(Dione^{Cl}Diolate)Rh(CO)_2]^-$ [51], mononuclear tris-ligand chromium(III) and iron(III) complexes $[Et_3NH]^+_3[(Dione^{Cl}Diolate)_3M]^{3-}$ (M = Fe, Cr) [52], and polymeric mixed-ligand chromium manganese complex [53]. In the mononuclear complexes, the trialkylammonium cation is bound to the carbonyl groups of the redox-active ligand (NH...O 1.987–2.388 Å).

The six-membered C(1–6) rings of both complexes are characterized by the quinoid type of bond distribution, the C(2)–C(3) and C(1)–C(6) bonds are shifted (by 0.07–0.19 Å) compared with other bonds in the C(1–6) rings. However, in complex **I**, carbonyl groups are located virtually in one plane (the O(3)–C(4)–C(5)–O(4) torsion angle is 2.14°), because of interaction with the triethylammonium cation, while in **II** · MeOH, the O(3)–C(4)–C(5)–O(4) torsion angle is 22.09°, which corresponds to this type of distortions in the molecules of various *o*-qui-

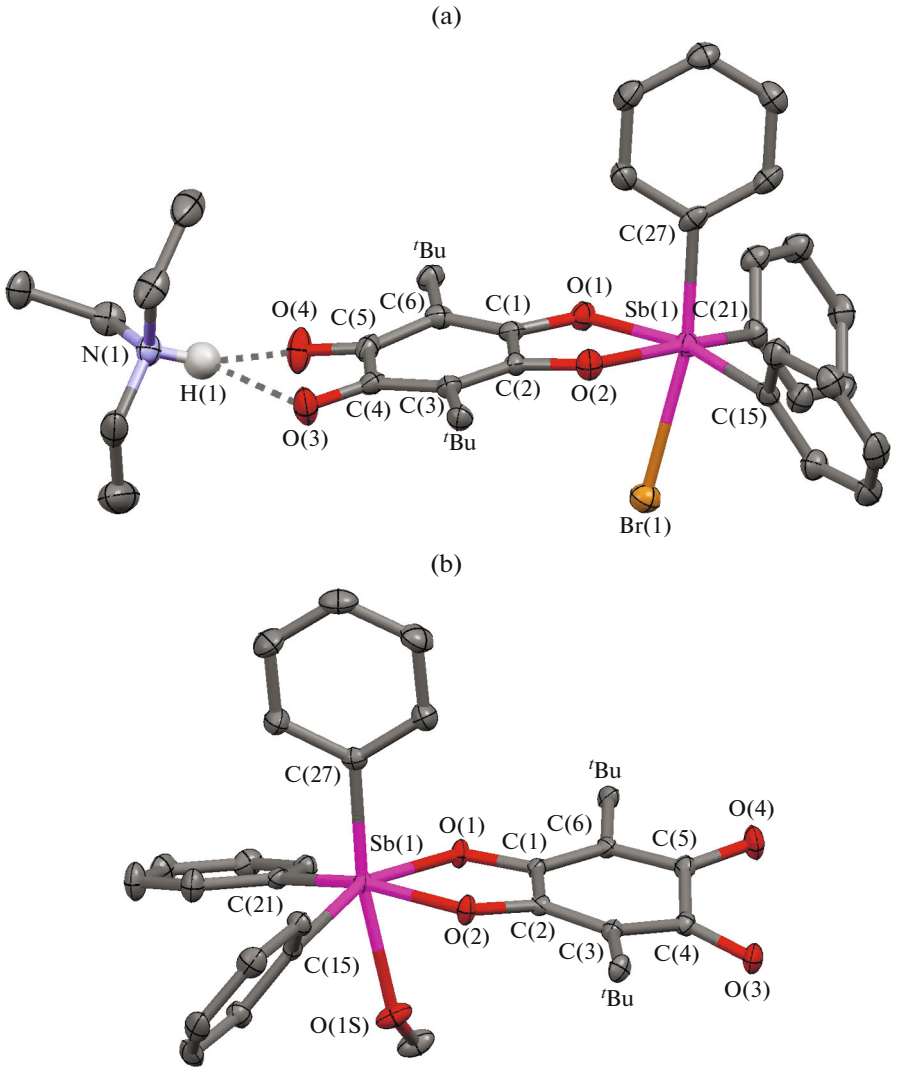

Fig. 1. Molecular structure of complexes in the crystals of (a) **I** · toluene and (b) **II** · 2MeOH (thermal ellipsoids at 50% probability level). The hydrogen atoms, except for those of the NH group, and methyl groups of the *tert*-butyl substituents are not shown.

nones [54]. Quite a lot of transition metal complexes based on unsubstituted 2,5-dihydoxy-*p*-benzoquinone and 3,6-dichloro- or 3,6-dinitro-2,5-dihydroxy-*p*-benzoquinone have been described in the literature. Among them are several mononuclear mono-, bis-, and tris-ligand derivatives in which free carbonyl groups are present in positions 4 and 5 of this redox-active diolate ligand, but the quinone moiety is less distorted: the O=C–C=O torsion angle usually does not exceed 6° [55–59].

In the crystal cell of **II** · 2MeOH, the **II** · MeOH molecules are arranged in such a way that they form dimers via the intermolecular hydrogen bonds with coordinated and solvated methanol molecules (Fig. 2). The corresponding distances are: O(1S)–H(1S)...O(2S), 1.78(1); O(2S)–H(2S)...O(3), 2.09(1); O(2S)–H(2S)...O(4), 2.50(1) Å; the angles are: (1S)H(1S)O(2S), 171.9(1)°; O(2S)H(2S)O(3), 147.5(1)°; O(2S)H(2S)O(4), 143.4(1)°.

The electrochemical behavior of complex **II** · MeOH was studied by cyclic voltammetry. Unlike most triarylantimony(V) catecholate complexes studied by this method [60–68], complex **II** · MeOH shows one irreversible single-electron oxidation peak at a high anodic potential of 1.44 V, corresponding to the formation of an unstable intermediate [**II** · MeOH]$^+$ (Scheme 3). The cathodic region exhibits a quasi-reversible single-electron reduction peak ($E_{1/2}$ = –1.52 V, Fig. 3), resulting in the generation of the radical anion form of the ligand in [**II** · MeOH]$^-$ (Scheme 3). The potential of this redox transition is considerably shifted to the cathodic region with respect to data for 3,6-di-*tert*-butyl-*o*-benzoquinone ($E_{1/2}$ = –0.51 V) obtained under analogous conditions. This potential shift attests to a decrease in the electron-withdrawing properties of the *o*-quinone moiety, which is due to the effect of the electron-donating catecholate metallacycle.

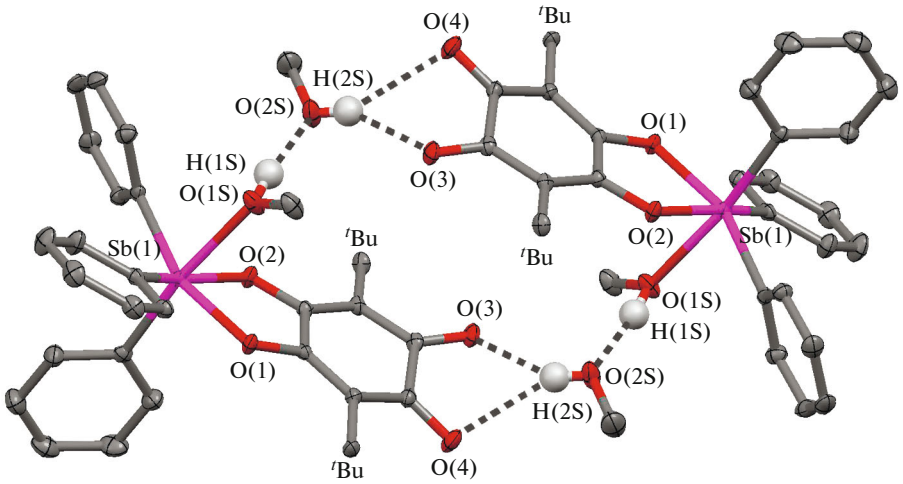

Fig. 2. Structure of the dimer in the crystals of **II** · 2MeOH (the *tert*-butyl groups and hydrogen atoms, except for the hydrogen atoms of the methanol OH groups, are not shown).

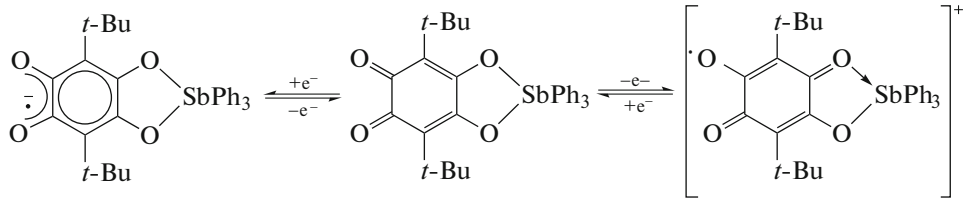

Scheme 3.

For comparison, the electrochemical reduction of *p*-benzoquinone Q$^{t\text{Bu}}$Diol in a dichloromethane proceeds in two steps, with the first wave being slightly reversible: E^1_{pc} = –0.26 V), which is associated with the subsequent chemical step: protonation of the generated radical anion by the neighboring quinone molecule, while the second reduction step (E^2_{pc} = –1.04 V ($E_{1/2}$ = –0.95 V)) is quasi-reversible (I_a/I_c = 0.8), which is due to reversibility: reduction of the resulting radical. The oxidation of this *p*-benzoquinone is irreversible and takes place at +1.80 V.

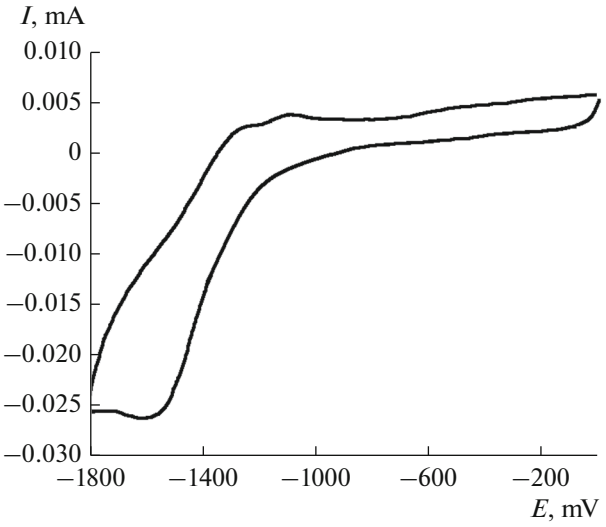

Fig. 3. CV reduction of complex **II** · MeOH in the potential sweep range from 0 to –1800 mV (CH_2Cl_2, glass carbon electrode, 0.15 M Bu_4NClO_4, c = 0.002 mol/L, V = 0.2 V/s versus Ag/AgCl/KCl(sat.)).

The electronic structure of compound **II** was also studied by DFT quantum chemical calculations, according to which the frontier orbitals responsible for the redox behavior of the complex are located in the redox-active ligand (HOMO = –5.7 eV, LUMO = 2.33 eV). The resulting energy gap (LUMO–HOMO = 3.37 eV) is in good agreement with the CV data. Unfortunately, attempts to prepare a binuclear triphenylantimony(V) complex from **II** or **II** · MeOH by an exchange or addition reaction have so far been unsuccessful. This is attributable to the decrease in the reduction potential of the *o*-quinone moiety in **II** · MeOH after attachment of triphenylantimony via oxygen atoms in positions 4 and 5 of formally 3,6-di-*tert*-butyl-*o*-benzoquinone compared with the initial ligand or *o*-quinones studied previously.

Thus, we studied the reactions of 2,5-dihydoxy-3,6-di-*tert*-butyl-*p*-benzoquinone with Ph_3SbBr_2 in the presence of triethylamine in toluene and methanol. In toluene, the reaction gives the ionic complex

$[Et_3NH]^+[(Dione^{tBu}Diolate)SbPh_3Br]^-$, which is actually the product of displacement of only one halogen atom from the antimony coordination sphere, while triethylamine completely deprotonates the redox-active ligand to give the triethylammonium cation and the (1,2-diolate)triphenylbromoantimonate(V) anion. In methanol, bromide ions are completely displaced from the coordination sphere of antimony to give the corresponding substituted triphenylantimony(V) 1,2-diolate ($Dione^{tBu}Diolate$)-$SbPh_3 \cdot MeOH$. According to X-ray diffraction data, both complexes are characterized by quinoid distortion of six-membered carbon ring and C=O double bonds in the $Ph_3SbO_2C_6(t\text{-}Bu)_2O_2$ moieties. Formally the complexes can be considered as 3,6-di-*tert*-butyl-*o*-benzoquinone derivatives with the Ph_3SbO_2 organometallic moiety attached to positions 4 and 5 of the quinone ring. The electrochemical reduction of the substituted triphenylantimony(V) 1,2-diolate in dichloromethane takes place at a large negative potential ($E_{1/2} = -1.52$ V), which attests to a considerable decrease in the electron-withdrawing properties of the *o*-quinone moiety due to the electron-donating effect of the catecholate metallacycle.

ACKNOWLEDGMENTS

The spectroscopic and X-ray diffraction studies were carried out using the equipment of the Center for Collective Use of the Razuvaev Institute of Organometallic Chemistry, Russian Academy of Sciences.

FUNDING

This work was carried out within the State Assignment of the Razuvaev Institute of Organometallic Chemistry, Russian Academy of Sciences.

CONFLICT OF INTEREST

The authors declare that they have no conflicts of interest.

REFERENCES

1. Loll, B., Kern, J., Saenger, W., et al., *Nature*, 2005, vol. 438, p. 1040.
2. Tsukihara, T., Aoyama, H., Yamashita, E., et al., *Science*, 1995, vol. 269, p. 1069.
3. Peters, J.W. and Szilagyi, R.K., *Curr. Opin. Chem. Biol.*, 2006, vol. 10, p. 101.
4. Corpas, F.J., Fernández-Ocña, A., Carreras, A., et al., *Plant Cell Physiol.*, 2006, vol. 47, p. 984.
5. Schenk, G., Ge, Y., Carrington, L., et al., *Arch. Biochem. Biophys.*, 1999, vol. 370, p. 183.
6. Adams, R.D. and Cotton, F.A., *Catalysis by Di- and Polynuclear Metal Cluster Complexes*, Wiley-VCH, 1998, p. 283.
7. Buchwalter, P., Rosé, J., and Braunstein, P., *Chem. Rev.*, 2015, vol. 115, p. 28.
8. Mata, J.A., Hahn, F.E., and Peris, E., *Chem. Sci.*, 2014, vol. 5, p. 1723.
9. Yalymov, A.I., Bilyachenko, A.N., Levitsky, M.M., et al., *Catalysts*, 2017, vol. 7, p. 1.
10. Kalck, P., *Top. Organomet. Chem.*, 2016, vol. 59, p. 1.
11. Molcanov, K., Juric, M., and Kojic-Prodic, B., *Dalton Trans.*, 2013, vol. 42, p. 15756.
12. Atzori, M., Artizzu, F., Marchio, L., et al., *Dalton Trans.*, 2015, vol. 44, p. 15786.
13. Simonson, A.N., Kareis, C.M., Ovanesyan, N.S., et al., *Polyhedron*, 2018, vol. 139, p. 215.
14. Kawata, S., Kumagai, H., Adachi, K., and Kitagawa, S., *Dalton Trans.*, 2000, p. 2409.
15. Bruijnincx, C.A., Viciano-Chumillas, M., Lutz, M., et al., *Chem.-Eur. J.*, 2008, vol. 14, p. 5567.
16. Benmansour, S., Gomez-Claramunt, P., Valles-Garcia, C., et al., *Cryst. Growth Des.*, 2016, vol. 16, p. 518.
17. Kil, Sik Min, Di Pasquale, A.G., Rheingold, A.L., et al., *J. Am. Chem. Soc.*, 2009, vol. 131, p. 6229.
18. Kil, Sik Min, Di Pasquale, A.G., Rheingold, A.L., et al., *Inorg. Chem.*, 2007, vol. 46, p. 1048.
19. Poddel'sky, A.I., *Nova Science Publishers*, Razeghi, M., Ed., New York, 2012, ch. 12, p. 267.
20. Cherkasov, V.K., Grunova, E.V., Poddel'sky, A.I., et al., *J. Organomet. Chem.*, 2005, vol. 690, p. 273.
21. Poddel'sky, A.I., Somov, N.V., Druzhkov, N.O., et al., *J. Organomet. Chem.*, 2011, vol. 696, no. 2, p. 517.
22. Kuropatov, V.A., Klement'eva, S.V., Poddel'sky, A.I., et al., *Russ. Chem. Bull. Int. Ed.,* 2010, vol. 59, no. 9, p. 1698.
23. Cherkasov, V.K., Grunova, E.V., and Abakumov, G.A., *Izv. Akad. Nauk, Ser. Khim.*, 2005, vol. 9, p. 2004.
24. Baryshnikova, S.V., Bellan, E.V., Poddel'sky, A.I., et al., *Eur. J. Inorg. Chem.*, 2016, vol. 33, p. 5230.
25. Gordon, A. and Ford, R., *The Chemist's Companion: A Handbook of Practical Data, Techniques, and References*, New York: Wiley, 1972.
26. Frisch, M.J., *Gaussian 09 (revision E.01)*, Wallingford: Gaussian, Inc., 2013.
27. *SAINT. Data Reduction and Correction Program. Version 8.27B*, Madison: Bruker AXS Inc., 2014.
28. CrysAlis Pro, Rigaku Oxford Diffraction, 2015.
29. Sheldrick, G.M., *SADABS-2012/1. Bruker/Siemens Area Detector Absorption Correction Program*, Madison: Bruker AXS Inc., 2012.
30. *SCALE3 ABSPACK: Empirical Absorption Correction. CrysAlis Pro-Software Package*, Agilent Technologies, 2012.
31. Sheldrick, G.M., *SHELXTL. Version6.14. Structure Determination Software Suite*, Madison: Bruker AXS, 2003.
32. Cherkasov, V.K., Abakumov, G.A., Grunova, E.V., et al., *Chem.-Eur. J.*, 2006, vol. 12, no. 14, p. 3916.
33. Poddel'sky, A.I., Smolyaninov, I.V., Kurskii, Yu.A., et al., *Russ. Chem. Bull. Int. Ed.*, 2009, vol. 58, no. 3, p. 532.
34. Poddel'sky, A.I., Vavilina, N.N., Somov, N.V., et al., *J. Organomet. Chem.*, 2009, vol. 694, no. 21, p. 3462.

35. Poddel'sky, A.I. and Smolyaninov, I.V., *Russ. J. Gen. Chem.*, 2010, vol. 80, no. 3, p. 538.
36. Poddel'sky, A.I., Smolyaninov, I.V., Berberova, N.T., et al., *J. Organomet. Chem.*, 2015, vols. 789–790, p. 8.
37. Poddel'sky, A.I., Arsenyev, M.V., Astaf'eva, T.V., et al., *J. Organomet. Chem.*, 2017, vol. 835, p. 17.
38. Poddel'sky, A.I., Okhlopkova, L.S., Meshcheryakova, I.N., et al., *Russ. J. Coord. Chem.*, 2019, vol. 45, p. 133. https://doi.org/10.1134/S1070328419010093
39. Hall, M. and Sowerby, D.B., *J. Am. Chem. Soc.*, 1980, vol. 102, no. 2, p. 628.
40. Holmes, R.R., Day, R.O., Chandrasekhar, V., and Holmes, J.M., *Inorg. Chem.*, 1987, vol. 26, p. 157.
41. Dodonov, V.A., Fedorov, A.Yu., Fukin, G.K., et al., *Main Group Chem.*, 1999, vol. 3, no. 1, p. 15.
42. Poddel'sky, A.I., Smolyaninov, I.V., Fukin, G.K., et al., *J. Organomet. Chem.*, 2018, vol. 867, p. 238.
43. Poddel'sky, A.I., Astaf'eva, T.V., Smolyaninov, I.V., et al., *J. Organomet. Chem.*, 2018, vol. 873, p. 57.
44. Arsenyev, M.V., Astaf'eva, T.V., Baranov, E.V., et al., *Mendeleev Commun.*, 2018, vol. 28, p. 76.
45. Poddel'sky, A.I., Druzhkov, N.O., Fukin, G.K., et al., *Polyhedron*, 2017, vol. 124, p. 41.
46. Poddel'sky, A.I., Smolyaninov, I.V., Fukin, G.K., et al., *J. Organomet. Chem.*, 2016, vol. 824, p. 1.
47. Poddel'sky, A.I., Ilyakina, E.V., Smolyaninov, I.V., et al., *Russ. Chem. Bull., Int. Ed.*, 2014, vol. 63, no. 4, p. 923.
48. Poddel'sky, A.I., Baranov, E.V., Fukin, G.K., et al., *J. Organomet. Chem.*, 2013, vol. 733, p. 44.
49. Poddel'sky, A.I., Somov, N.V., Druzhkov, N.O., et al., *J. Organomet. Chem.*, 2011, vol. 696, no. 2, p. 517.
50. Lide, D.R., *CRC Handbook of Chemistry and Physics*, CRC Press: Boca-Raton, 2005, p. 513.
51. Elduque, A., Garces, Y., Lahoz, F.J., et al., *Inorg. Chem. Commun.*, 1999, vol. 2, p. 414.
52. Atzori, M., Artizzu, F., Sessini, E., et al., *Dalton Trans.*, 2014, vol. 43, p. 7006.
53. Palacios-Corella, M., Fernandez-Espejo, A., Bazaga-Garcia, M., et al., *Inorg. Chem.*, 2017, vol. 56, p. 13865.
54. Fukin, G.K., Cherkasov, A.V., Shurygina, M.P., et al., *Struct. Chem.*, 2010, vol. 21, no. 3, p. 607.
55. Folgado, J.V., Ibanez, R., Coronado, E., et al., *Inorg. Chem.*, 1988, vol. 27, p. 19.
56. Spengler, R., Lange, J., Zimmermann, H., et al., *Acta Crystallogr., Sect. B: Struct. Sci.*, 1995, vol. 51, p. 174.
57. Nagayoshi, K., Kabir, Md.K., Tobita, H., et al., *J. Am. Chem. Soc.*, 2003, vol. 125, p. 221.
58. Ishikawa, R., Horii, Y., Nakanishi, R., et al., *Eur. J. Inorg. Chem.*, 2016, p. 3233.
59. Dubraja, L., Molcanov, K., Zilic, D., et al., *New J. Chem.*, 2017, vol. 41, p. 6785.
60. Poddel'sky, A.I., Smolyaninov, I.V., Somov, N.V., et al., *J. Organomet. Chem.*, 2010, vol. 695, no. 4, p. 530.
61. Poddel'sky, A.I., Smolyaninov, I.V., Kurskii, Yu.A., et al., *J. Organomet. Chem.*, 2010, vol. 695, no. 8, p. 1215.
62. Smolyaninov, I.V., Poddel'skiy, A.I., Berberova, N.T., et al., *Russ. J. Coord. Chem.*, 2010, vol. 36, no. 9, p. 644. https://doi.org/10.1134/S1070328410090022
63. Poddel'sky, A.I., Smolyaninov, I.V., Vavilina, N.N., et al., *Russ. J. Coord. Chem.*, 2012, vol. 38, no. 4, p. 284. https://doi.org/10.1134/S1070328412040094
64. Poddel'sky, A.I., Arsen'ev, M.V., Okhlopkova, L.S., et al., *Russ. J. Coord. Chem.*, 2017, vol. 43, no. 12, p. 843. https://doi.org/10.1134/S1070328417120089
65. Smolyaninov, I.V., Antonova, N.A., Poddel'sky, A.I., et al., *Appl. Organomet. Chem.*, 2012, vol. 26, no. 6, p. 277.
66. Smolyaninova, S.A., Poddel'sky, A.I., Smolyaninov, I.V., and Berberova, N.T., *Russ. J. Coord. Chem.*, 2014, vol. 40, no. 5, p. 273. https://doi.org/10.1134/S107032841405011X
67. Smolyaninov, I.V., Poddel'skii, A.I., Smolyaninova, S.A., and Movchan, N.O., *Russ. J. Gen. Chem.*, 2014, vol. 84, no. 9, p. 1761.
68. Smolyaninov, I.V., Poddel'skii, A.I., Smolyaninova, S.A., and Berberova, N.T., *Russ. J. Electrochem.*, 2015, vol. 51, no. 11, p. 1021.

Translated by Z. Svitanko